**Reprinted from**

# Chemical Physics

---

Chemical Physics 195 (1995) 117–127

# A theoretical study on the ionic states, with analysis of vibrational levels of the photoelectron spectrum, of formic acid ($CH_2O_2$ and $CD_2O_2$)

Kouichi Takeshita

*Faculty of Bioindustry, Tokyo University of Agriculture, Abashiri, Hokkaido 099-24, Japan*

Received 24 January 1994; in final form 9 January 1995

N·H

ELSEVIER

# CHEMICAL PHYSICS

*A journal devoted to experimental and theoretical research involving problems of both a chemical and a physical nature*

## EDITORS

ROBIN M. HOCHSTRASSER
Department of Chemistry, University of Pennsylvania,
Philadelphia, PA 19104-6323, USA
FAX 1-215-8980590

G. LUDWIG HOFACKER
Lehrstuhl für Theoretische Chemie, Technische Universität München,
Lichtenbergstrasse 4, 85747 Garching, Germany
FAX 49-89-32093622

## ASSOCIATE EDITORS

DAVID CHANDLER, Department of Chemistry, University of California Berkeley, Berkeley, CA 94720, USA. FAX 1-510-6428369
H. PETER TROMMSDORFF, Laboratoire de Spectrométrie Physique, Université Joseph-Fourier Grenoble I, B.P. 87, 38402 Saint-Martin-d'Hères Cedex, France. FAX 33-76-514544

## ADVISORY EDITORIAL BOARD

*Australia*
D.P. CRAIG, Canberra
N.S. HUSH, Sydney

*Canada*
J.C. POLANYI, Toronto

*Czech Republic*
Z. HERMAN, Prague

*Denmark*
G.D. BILLING, Copenhagen

*France*
S. LEACH, Orsay
J.L. MARTIN, Palaiseau
A. TRAMER, Orsay

*Germany*
H. BÄSSLER, Marburg
B. DICK, Regensburg
S.F. FISCHER, Garching
H. GRABERT, Freiburg
D. HAARER, Bayreuth
P. HÄNGGI, Augsburg
W. LORENZ, Leipzig
D. MENZEL, Garching
E.W. SCHLAG, Garching
W. ZINTH, Munich

*Hungary*
P. ORMOS, Szeged

*Israel*
A.I. BURSHTEIN, Rehovot
J. JORTNER, Tel Aviv
R.D. LEVINE, Jerusalem
M. SHAPIRO, Rehovot

*Italy*
M. CAPITELLI, Bari

*Japan*
H. HAMAGUCHI, Kawasaki
T. KITAGAWA, Okazaki
T. KOBAYASHI, Tokyo
S. NAGAKURA, Yokohama
K. YOSHIHARA, Okazaki

*The Netherlands*
D. FRENKEL, Amsterdam

*Russian Federation*
V.S. LETOKHOV, Moscow

*Sweden*
R. RIGLER, Stockholm
K. SIEGBAHN, Uppsala

*Switzerland*
H. FISCHER, Zurich
J.P. MAIER, Basel

*Taiwan*
Y.T. LEE, Taipei

*United Kingdom*
A.D. BUCKINGHAM, Cambridge
D.A. KING, Cambridge
P.A. MADDEN, Oxford
J.P. SIMONS, Oxford

*USA*
A.C. ALBRECHT, Ithaca, NY
H.C. ANDERSEN, Stanford, CA
P.F. BARBARA, Minneapolis, MN
R. BERSOHN, New York, NY
S.G. BOXER, Stanford, CA
K.A. DILL, San Francisco, CA
M.D. FAYER, Stanford, CA
G.R. FLEMING, Chicago, IL
G. FLYNN, New York, NY
R.A. FRIESNER, New York, NY
C.B. HARRIS, Berkeley, CA
E.J. HELLER, Cambridge, MA
B. HUDSON, Eugene, OR
M. KLEIN, Philadelphia, PA

*USA (continued)*
W.C. LINEBERGER, Boulder, CO
D.S. McCLURE, Princeton, NJ
W.H. MILLER, Berkeley, CA
M.D. NEWTON, Upton, NY
C.S. PARMENTER, Bloomington, IN
A. PINES, Berkeley, CA
W. PLUMMER, Philadelphia, PA
M.A. RATNER, Evanston, IL
G.W. ROBINSON, Lubbock, TX
G.J. SMALL, Ames, IA
J.D. WEEKS, College Park, MD
P.G. WOLYNES, Urbana, IL
R.N. ZARE, Stanford, CA
A.H. ZEWAIL, Pasadena, CA

*Important: please adhere to instructions to authors, to be found on the last pages of each volume.*

After acceptance of the paper for publication, further correspondence should be sent to the publishers (Drs. H.A. Arends, Editorial Department, Chemistry & Chemical Engineering Department, P.O. Box 330, 1000 AH Amsterdam, The Netherlands; FAX 31-20-4852459; telex 10704 espom nl; electronic mail X400: C=NL; A=400NET; P=SURF; O=ELSEVIER; S=ARENDS, I=H or RFC822: H.ARENDS@ELSEVIER.NL).

*Publication information. Chemical Physics* (ISSN 0301-0104). For 1995 volumes 188–200 are scheduled for publication. Subscription prices are available upon request from the publisher. Subscriptions are accepted on a prepaid basis only and are entered on a calendar year basis. Issues are sent by surface mail except to the following countries where air delivery via SAL is ensured: Argentina, Australia, Brazil, Canada, Hong Kong, India, Israel, Japan, Malaysia, Mexico, New Zealand, Pakistan, PR China, Singapore, South Africa, South Korea, Taiwan, Thailand, USA. For all other countries airmail rates are available upon request. Claims for missing issues must be made within six months of our publication (mailing) date. Please address all your requests regarding orders and subscription queries to: Elsevier Science B.V., Journal Department, P.O. Box 211, 1000 AE Amsterdam, The Netherlands. Tel.: (+31-20)485-3642, Fax: (+31-20)485-3598.

*US mailing notice. Chemical Physics* (ISSN 0301-0104) is published semi-monthly by Elsevier Science (Molenwerf 1, P.O. Box 211, 1000 AE Amsterdam). Annual subscription price in the USA US$ 3353.00, including air speed delivery, valid in North, Central and South America only. Second class postage paid at Jamaica, NY 11431.
USA POSTMASTERS: Send address changes to: Chemical Physics, Publications Expediting, Inc., 200 Meacham Avenue, Elmont, NY 11003. Airfreight and mailing in the USA by Publication Expediting.

*Information for Advertisers.* Advertising orders and enquiries can be sent to the Advertising Department, Elsevier Science B.V., P.O. Box 211, 1000 AE Amsterdam, The Netherlands. Tel.: (+31-20 ) 485-3796; Fax: (+31-20) 485-3810. Courier shipments to street addresses: Molenwerf 1, 1014 AG Amsterdam, The Netherlands.
For Great Britain: TG Scott & Son Ltd., Vanessa Bird, Portland House 21, Narborough Road, Cosby, Leicestershire LE9 5TA. Tel: (44-116) 2750-521/2753-333; Fax: (+44-116) 2750-522.
For USA & Canada: Weston Media Associates, Daniel Lipner, P.O. Box 1110, Greens Farms, CT 06436-1110. Tel: (+1-203) 261-2500; Fax: (+1-203) 261-0101.

Printed in The Netherlands

Published semi-monthly

ELSEVIER

Chemical Physics 195 (1995) 117–127

Chemical Physics

# A theoretical study on the ionic states, with analysis of vibrational levels of the photoelectron spectrum, of formic acid ($CH_2O_2$ and $CD_2O_2$)

Kouichi Takeshita

*Faculty of Bioindustry, Tokyo University of Agriculture, Abashiri, Hokkaido 099-24, Japan*

Received 24 January 1994; in final form 9 January 1995

## Abstract

Ab initio calculations are performed to study the molecular equilibrium structures and the vibrational levels of the low-lying $^2A'$ and $^2A''$ states of formic acid ($CH_2O_2$). The theoretical intensity curves obtained by the Franck–Condon factors for ionization transitions are also reported and compared with the photoelectron spectra of $CH_2O_2$ and $CD_2O_2$. Some new assignments of the vibrational levels of the photoelectron spectrum are proposed.

## 1. Introduction

The electronic ground state ($^1A'$) of formic acid is represented by a configuration of $\ldots(1a'')^2(9a')^2(2a'')^2(10a')^2$ with the $C_s$ symmetry point group.

The photoelectron (PE) spectrum of $CH_2O_2$ has been observed in the 11.3–13 eV region where two bands of the $^2A'$ and $^2A''$ states have been found [1–5]. These bands show vibrational fine structure. The assignment of the vibrational fine structure has been discussed [1–4]. Watanabe et al. [3] have reported the vibrational frequencies for formic acid deuterium derivative cations. They assigned the vibrational structure by using the vibrational modes of the ground state.

As a molecule is ionized, the equilibrium molecular structure, the characters of the vibrational modes and the vibrational frequencies change from those of the ground state. The vibrational structure of the PE spectrum reflects these changes. It is, therefore, interesting to investigate the vibrational structure associated with the changes in the equilibrium molecular structure and vibrational modes by ionization. Ab initio investigations on the equilibrium molecular structure of the $^1A'$, $^2A'$ and $^2A''$ states have been reported concerning the study of the 1,3-hydrogen migration [6,7]. Vibrational frequencies of the ground state were reported [8,9]. However, no theoretical study on the vibrational fine structure of the PE spectrum has been reported.

In this work, we determine the equilibrium molecular structures of the ground state and the ionic states by using the ab initio method. Within the framework of the adiabatic approximation and the harmonic oscillator approximation, we calculate the harmonic force constant matrix elements over variables of the totally symmetric distortion and vibrational frequencies of the seven totally symmetric modes ($\nu_1$–$\nu_7$). We obtaine the approximate theoretical intensity curve using the Franck–Condon factor (FCF). Bas-

*SSDI* 0301-0104(95)00033-X

ing on these calculations, we discuss the vibrational fine structures of the ionic states in comparison with the PE spectra of $CH_2O_2$ and $CD_2O_2$.

## 2. Method of calculations

We used the basis sets of the MIDI-4-type prepared by Tatewaki and Huzinaga [10]. These were augmented by one p-type polarization function for H and one d-type polarization function for C and O. The exponents of the polarization function for H, C and O are 0.68, 0.61 and 1.16, respectively.

The gradient technique for the Roothaan's restricted Hartree–Fock (RHF) method was applied to find the optimum molecular structure. The single and double excitation configuration interaction (SDCI) method was used to get more accurate ionization energies for the estimation of vertical ionization energies (VIEs) and adiabatic ionization energies (AIEs). A single reference configuration of the SCF wave function of the respective state was used. In the SDCI method, singly and doubly excited configuration state functions (CSFs) were generated where the inner shells (K shells of C and O) were kept frozen. The generated CSFs were then restricted to the first order interacting space [11]. The number of the generated CSFs of the $^1A'$, $^2A'$ and $^2A''$ states were 34401, 35523 and 35118, respectively. As the dimensions of the SDCI were too large, we have adopted a CSF selection process by the second-order perturbation theory. A threshold for the selection was 5 $\mu$hartree. We have estimated the total energy including the contribution from the rejected CSFs by the second-order perturbation theory [12].

The totally symmetric harmonic force constant matrix elements were calculated by the gradient technique within the framework of the RHF method. The second derivative was estimated by numerical differentiation of the first derivative. We calculated the FCFs only for the totally symmetric modes. The method of calculation of the FCF and theoretical intensity curve was the same as the one used in our previous study [13].

This work was carried out by using the computer program system GRAMOL [14] for the gradient technique and the calculation of normal modes. The calculations of the FCF and the theoretical intensity curve were done by the program system FCF&TIC [16]. The program MICA3 [17] was used for the CI calculations.

## 3. Results and discussion

A geometrical optimization of the cis and trans conformations of the ground state was performed. The trans conformation was more stable than the cis conformation by 5.6 kcal/mol at the RHF level. A rotational barrier height between the cis and trans

Table 1
Optimized geometry

| | $^1A'$ | | $^2A'$ | $^2A''$ |
|---|---|---|---|---|
| | calc. | exp. [a] | | |
| C–H | 1.094 | 1.097 | 1.091 (−0.003) | 1.088 (−0.006) |
| C–O$_1$ | 1.179 | 1.204 | 1.257 (0.078) | 1.327 (0.148) |
| C–O$_2$ | 1.321 | 1.342 | 1.243 (−0.078) | 1.224 (−0.097) |
| O–H | 0.952 | 0.972 | 0.964 (0.012) | 0.969 (0.018) |
| O$_1$–C–H | 124.76 | 123.2 | 116.61 (−8.15) | 121.35 (−3.41) |
| O$_1$–C–O$_2$ | 124.91 | 124.8 | 123.86 (1.05) | 120.36 (−4.55) |
| C–O$_2$–H | 108.41 | 106.3 | 117.22 (8.81) | 115.67 (7.26) |

[a] Ref. [18].

Bond lengths are in angstroms, angles in degrees. The values in parentheses are the magnitude of the change in geometry by ionization. Nguyen et al. [6,7] reported the following optimized geometries by using the UHF/6-31G** method: For $^1A'$, C–H = 1.085, C–O$_1$ = 1.182, C–O$_2$ = 1.322, O–H = 0.949, O$_1$–C–H = 124.6, O$_1$–C–O$_2$ = 124.9 and C–O$_2$–H = 108.9. For $^2A'$, C–H = 1.083, C–O$_1$ = 1.260, C–O$_2$ = 1.245, O–H = 0.960, O$_1$–C–H = 116.8, O$_1$–C–O$_2$ = 123.7 and C–O$_2$–H = 118.5. For $^2A''$, C–H = 1.079, C–O$_1$ = 1.322, C–O$_2$ = 1.231, O–H = 0.967, O$_1$–C–H = 122.8, O$_1$–C–O$_2$ = 119.7 and C–O$_2$–H = 116.5.

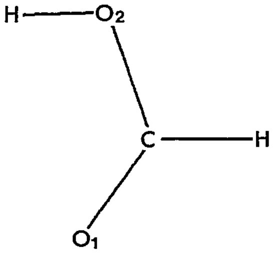

Fig. 1. The numbering of each atom.

conformations was estimated. It was 14.0 kcal/mol. Considering the Boltzmann distribution low, the probability of existence of the cis conformation at room temperature is less than $1.0 \times 10^{-4}$ %. Therefore, the observed PE spectrum should originate from the trans conformation. It should be reasonable to consider only the trans conformation on the theoretical study of the PE spectrum. The geometrical parameters of the optimized molecular structures and the experimental values [18] are listed in Table 1. Fig. 1 shows the numbering of each atom. In the ground state the $C-O_1$ and $C-O_2$ bonds have double and single bond characters, respectively. The differences of the geometrical parameters between the ionic and ground states are given in parenthesis in Table 1. An appreciable geometrical change is found at both states in the bond lengths of $C-O_1$ and $C-O_2$, the bond angles of $O_1-C-H$, $O_1-C-O_2$ and $C-O_2-H$. The C=O double bond lengthens and the C–O single bond shortens by ionization. We notice that the bond length of $C-O_1$ becomes longer than that of $C-O_2$. The calculated each bond length of $C-O_1$ and $C-O_2$ of $^2A'$ is nearly equal to the average length of the single and double bond in the ground state. Thus, the distinction of characters of the single and double bond should be meaningless in the ionic states. The present calculations of the $^1A'$, $^2A'$ and $^2A''$ states are in good agreement with another calculation at the UHF/6-31G** level by Nguyen et al. [6–7] of which the result is given in the footnote of Table 1.

The VIEs and AIEs were calculated. In the present calculations, the VIE is obtained by the difference of the two energies between the ground state and the ionic state using the geometry of the ground state. The AIE is estimated from the difference energies of the optimized structures of the ground and ionic states. The results are shown in Table 2. In the SDCI calculations the weight of each reference function of the $^1A'$, $^2A'$ and $^2A''$ states at the optimized geometries are 89.9, 90.0, and 89.3%, respectively. The weight of each CSF other than the reference CSF is less than 1%. Therefore, the RHF approximation method should be the same level for the $^1A'$, $^2A'$ and $^2A''$ states. The energy lowering of the AIE of the $^2A'$ and $^2A''$ states from the VIE by the SDCI calculations are 0.36 and 0.81 eV, respectively. Kimura et al. [5] reported the observed VIE. The observed VIEs of the $^2A'$ and $^2A''$ states were 10.87 and 12.05 eV, respectively. The VIEs by the SDCI calculation are 10.88 and 12.44 eV for the $^2A'$ and $^2A''$ states, respectively. The observed VIE is defined as the energy to ionize a molecule from the zero point vibrational level of the ground state to the vibrationally excited levels of the positive ion with maximum photoionization probabilities. Therefore, the observed VIE does not always correspond to the calculated VIE. It is more reasonable to compare the calculated zero–zero (0–0) IE to the observed 0–0 IE. Using the AIEs by the SDCI calculation and the zero point vibrational energies, we estimate the 0–0 IEs. The 0–0 IEs of the $^2A'$ and $^2A''$ states of $CH_2O_2$ are 10.47 and 11.56 eV, respectively. We also calculated the FCFs of the 0–0 transition. The FCFs of the $^2A'$ and $^2A''$ states of $CH_2O_2$ are 0.12 and 0.009, respectively. The FCF of the $^2A'$ state is so large that

Table 2
Ionization energies (eV)

| State | VIE | | AIE | | Δ (VIE – AIE) | | 0–0 transition | |
|---|---|---|---|---|---|---|---|---|
| | SCF | SDCI | SCF | SDCI | SCF | SDCI | 0–0 IE | FCF |
| $^2A'$ | 10.11 | 10.88 | 9.66 | 10.52 | 0.45 | 0.36 | 10.47 | 0.123 |
| $^2A''$ | 11.70 | 12.44 | 10.70 | 11.63 | 1.00 | 0.81 | 11.56 | 0.009 |

VIE: Vertical ionization energy; AIE: Adiabatic ionization energy. Total energy (au) of $^1A'$: −188.570787 (SCF) and −189.027513 (SDCI). The observed VIEs of the $^2A'$ and $^2A''$ states were 10.87 and 12.05 eV, respectively [5]. The observed 0–0 IE of the $^2A'$ state was 11.33 eV [4].

the 0–0 transitions should be observed. The observed 0–0 IE of the first ionic states was 11.33 eV [4]. The calculated value is underestimated by 0.86 eV.

Tables 3 and 4 contain the calculated vibrational frequencies of the total symmetric modes of $CH_2O_2$ and $CD_2O_2$, respectively. The vibrational modes from $\nu_1$ to $\nu_7$ are ordered by the magnitude of frequencies. The calculated vibrational frequencies of the $^1A'$ state are compared with the observed values [19]. The calculated values are overestimated by 9–15%. Chang et al. [8] have reported the calculated vibrational frequencies using the double-$\zeta$ plus polarization (DZ + P) basis. Williams and Lowrey [9] have obtained the calculated frequencies using the 4–31G basis. The present calculated frequencies are in good agreement with those by Chang et al., whose result is given in the footnote of Table 2. A potential energy distribution (PED) [20] was calculated in order to characterize each normal mode. The results are shown in Tables 3 and 4. Each normal mode is also characterized by using the classical half-amplitude of the zero-point vibrational level shown in Tables 5 and 6. We note that the overall sign is arbitrary for each motion.

For the $^1A'$ state of $CH_2O_2$, Table 3 shows that the $\nu_1$, $\nu_2$, $\nu_3$ and $\nu_6$ modes may be characterized as the O–H, C–H, C–$O_1$ and C–$O_2$ stretching modes, respectively. The $\nu_4$, $\nu_5$ and $\nu_7$ modes should be assigned to the $O_1$–C–H, C–$O_2$–H and $O_1$–C–$O_2$ bending modes, respectively. Millikan and Pitzer [21] assigned the character of each vibrational mode. We show their assignment in the footnote of Table 3. Our assignment is consistent with their assignment.

For the $^2A'$ state of $CH_2O_2$, the characters of the $\nu_1$, $\nu_2$ and $\nu_7$ modes are the same as those of the ground state. However, the characters of the $\nu_3$, $\nu_4$,

Table 3
Vibrational frequencies ($cm^{-1}$) and potential energy distributions of $CH_2O_2$

| | Calc. | Obs. [a] | Potential energy distribution (%) |
|---|---|---|---|
| $^1A'$ | | | |
| $\nu_1$ | 4082 | 3569 | O–H (100) |
| $\nu_2$ | 3269 | 2942 | C–H (98) |
| $\nu_3$ | 2033 | 1777 | C–$O_1$ (83), C–$O_2$ (8), $O_1$–C–H (5), C–$O_2$–H (3) |
| $\nu_4$ | 1528 | 1381 | $O_1$–C–H (87), C–$O_1$ (5), C–$O_2$–H (5) |
| $\nu_5$ | 1435 | 1223 | C–$O_2$–H (46), C–$O_2$ (22), $O_1$–C–$O_2$ (16), $O_1$–C–H (15) |
| $\nu_6$ | 1276 | 1104 | C–$O_2$ (62), C–$O_2$–H (30), $O_1$–C–H (3), $O_1$–C–$O_2$ (3) |
| $\nu_7$ | 697 | 625 | $O_1$–C–$O_2$ (76), C–$O_2$–H (12), $O_1$–C–H (8), C–$O_2$ (4) |
| $^2A'$ | | | |
| $\nu_1$ | 3918 | | O–H (100) |
| $\nu_2$ | 3335 | | C–H (99) |
| $\nu_3$ | 1796 | | C–$O_2$ (50), C–$O_1$ (32), $O_1$–C–H (16) |
| $\nu_4$ | 1527 | | C–$O_2$ (37), C–$O_2$–H (22), C–$O_1$ (18), $O_1$–C–$O_2$ (13), $O_1$–C–H (9) |
| $\nu_5$ | 1326 | | $O_1$–C–H (56), C–$O_1$ (40) |
| $\nu_6$ | 1281 | | C–$O_2$–H (71), $O_1$–C–H (16), C–$O_2$ (9), C–$O_1$ (4) |
| $\nu_7$ | 605 | | $O_1$–C–$O_2$ (77), $O_1$–C–H (19), C–$O_2$–H (3) |
| $^2A''$ | | | |
| $\nu_1$ | 3841 | | O–H (100) |
| $\nu_2$ | 3380 | | C–H (99) |
| $\nu_3$ | 1844 | | C–$O_2$ (60), $O_1$–C–H (18), C–$O_2$–H (12), C–$O_1$ (9) |
| $\nu_4$ | 1527 | | $O_1$–C–$O_2$ (54), $O_1$–C–H (25), C–$O_2$–H (11), C–$O_1$ (6), C–$O_2$ (3) |
| $\nu_5$ | 1363 | | $O_1$–C–H (48), $O_1$–C–$O_2$ (27), C–$O_2$–H (15), C–$O_1$ (11) |
| $\nu_6$ | 1226 | | C–$O_1$ (52), C–$O_2$–H (40), C–$O_2$ (5) |
| $\nu_7$ | 642 | | $O_1$–C–H (42), $O_1$–C–$O_2$ (36), C–$O_2$–H (16), C–$O_1$ (4) |

[a] Ref. [19].

Assignment of vibrational mode by Millikan and Pitzer [21] is as follows: $\nu_1$(O–H str.), $\nu_2$(C–H str.), $\nu_3$(C=O str.), $\nu_4$(C–H bend.), $\nu_6$(O–H bend.), $\nu_6$(C–O str.), and $\nu_7$(O–C–O bend.). Chang et al. [8] obtained the following frequencies of $^1A'$ from DZ + P SCF theory: $\nu_1 = 4116$, $\nu_2 = 3293$, $\nu_3 = 2015$, $\nu_4 = 1536$, $\nu_5 = 1426$, $\nu_6 = 1268$ and $\nu_7 = 690$ $cm^{-1}$.

$\nu_5$ and $\nu_6$ modes are quite different from those of the ground state. This situation should be a connection that the bond length of C–$O_2$ becomes shorter than that of C–$O_1$.

For the $^2A''$ state of $CH_2O_2$, the characters of the $\nu_1$ and $\nu_2$ modes are the same as those of the ground state. The characters of the other modes are quite different from those of the ground state. The change in the C–$O_2$ and C–$O_1$ bond lengths is more appreciable compared to that of the $^2A'$ state. This effect appears in the characters of the $\nu_3$ and $\nu_6$ modes.

For the $^1A'$ state of $CD_2O_2$, the $\nu_1$, $\nu_2$, $\nu_3$ and $\nu_6$ modes should be assigned to the O–D, C–D, C–$O_1$ and C–$O_2$ stretching modes, respectively. The $\nu_4$, $\nu_5$ and $\nu_7$ modes are assigned to the $O_1$–C–D, C–$O_2$–D, and $O_1$–C–$O_2$ bending modes, respectively. The present assignment is also consistent with that by Millikan and Pitzer.

The characters of the $\nu_1$, $\nu_2$, $\nu_5$ and $\nu_7$ modes of the $^2A'$ state of $CD_2O_2$ should correspond to each mode of the ground state. The character of the $\nu_6$ mode corresponds to that of the $\nu_4$ mode of the ground state. The characters of the $\nu_3$ and $\nu_4$ modes are a strong mixture of the C–$O_1$ and C–$O_2$ stretching motions. Table 6 shows that the $\nu_3$ and $\nu_4$ modes are the out-of-phase and in-phase modes of the C–$O_1$ and C–$O_2$ stretching motions, respectively.

The characters of the $\nu_1$ and $\nu_2$ modes of the $^2A''$ state of $CD_2O_2$ correspond to each mode of the ground state. The character of the $\nu_3$ mode corresponds with that of the $\nu_6$ mode of the ground state.

Fig. 2 shows the theoretical intensity curve (TIC) of the $^2A'$ state of $CH_2O_2$ and $CD_2O_2$ with a half-width of 300 $cm^{-1}$ and the observed PE spectrum (PES) from Watanabe et al. [3]. The vibrational structure of the TIC is in good agreement with that of the observed PES.

Table 6 shows the assignment of the vibrational

Table 4
Vibrational frequencies ($cm^{-1}$) and potential energy distributions of $CD_2O_2$

| | Calc. | Obs. [a] | Potential energy distribution (%) |
|---|---|---|---|
| $^1A'$ | | | |
| $\nu_1$ | 2970 | 2632 | O–D (100) |
| $\nu_2$ | 2440 | 2232 | C–D (87), C–$O_1$ (9), $O_1$–C–$O_2$ (3) |
| $\nu_3$ | 1989 | 1735 | C–$O_1$ (78), C–$O_2$ (10), C–D (6), $O_1$–C–D (4) |
| $\nu_4$ | 1335 | 1170 | $O_1$–C–D (64), C–$O_2$–D (19), C–$O_2$ (13), $O_1$–C–$O_2$ (4) |
| $\nu_5$ | 1148 | 1042 | C–$O_2$–D (62), $O_1$–C–D (17), $O_1$–C–$O_2$ (16), C–$O_1$ (4) |
| $\nu_6$ | 1060 | 945 | C–$O_2$ (60), $O_1$–C–D (23), $O_1$–C–$O_2$ (14) |
| $\nu_7$ | 618 | 556 | $O_1$–C–$O_2$ (66), C–$O_2$–D (27), $O_1$–C–D (4), C–$O_2$ (3) |
| $^2A'$ | | | |
| $\nu_1$ | 2857 | | O–D (99) |
| $\nu_2$ | 2477 | | C–D (94), C–$O_2$ (2), $O_1$–C–$O_2$ (2) |
| $\nu_3$ | 1774 | | C–$O_2$ (54), C–$O_1$ (35), $O_1$–C–D (9) |
| $\nu_4$ | 1409 | | C–$O_1$ (49), C–$O_2$ (44), $O_1$–C–D (11), C–D (4) |
| $\nu_5$ | 1066 | | C–$O_2$–D (60), $O_1$–C–D (19), C–$O_1$ (13), $O_1$–C–$O_2$ (7) |
| $\nu_6$ | 965 | | $O_1$–C–D (65), C–$O_2$–D (28), $O_1$–C–$O_2$ (4) |
| $\nu_7$ | 554 | | $O_1$–C–$O_2$ (73), $O_1$–C–D (17), C–$O_2$–D (10) |
| $^2A''$ | | | |
| $\nu_1$ | 2801 | | O–D (99) |
| $\nu_2$ | 2521 | | C–D (94), C–$O_2$ (3) |
| $\nu_3$ | 1819 | | C–$O_2$ (65), C–$O_1$ (12), $O_1$–C–D (11), $O_1$–C–$O_2$ (9) |
| $\nu_4$ | 1341 | | C–$O_1$ (53), $O_1$–C–$O_2$ (28), C–$O_2$–D (7), C–$O_2$ (6), C–D (3) |
| $\nu_5$ | 1068 | | $O_1$–C–$O_2$ (44), $O_1$–C–D (31), C–$O_1$ (13), C–$O_2$–D (12) |
| $\nu_6$ | 1013 | | $O_1$–C–D (49), $O_1$–C–$O_2$ (26), C–$O_2$–D (23) |
| $\nu_7$ | 576 | | C–$O_2$–D (35), $O_1$–C–$O_2$ (33), $O_1$–C–D (29) |

[a] Ref. [19].

Assignment of vibrational mode by Millikan and Pitzer [21] is as follows: $\nu_1$(O–D str.), $\nu_2$(C–D str.), $\nu_3$(C=O str.), $\nu_4$(C–D bend.), $\nu_6$(O–D bend.), $\nu_6$(C–O str.), and $\nu_7$(O–C–O bend.). Chang et al. [8] obtained the following frequencies of $^1A'$ from DZ + P SCF theory: $\nu_1 = 2996$, $\nu_2 = 2456$, $\nu_3 = 1983$, $\nu_4 = 1328$, $\nu_5 = 1145$, $\nu_6 = 1061$ and $\nu_7 = 611$ $cm^{-1}$.

Table 5
Classical half-amplitude of the zero-point vibrational level

| | $\nu_1$ | $\nu_2$ | $\nu_3$ | $\nu_4$ | $\nu_5$ | $\nu_6$ | $\nu_7$ |
|---|---|---|---|---|---|---|---|
| $CH_2O_2$ | | | | | | | |
| $^1A'$ state | | | | | | | |
| C–H | −0.001 | 0.105 | 0.004 | 0.003 | 0.002 | 0.000 | 0.000 |
| C–O$_1$ | 0.000 | −0.006 | 0.048 | 0.010 | −0.004 | −0.006 | 0.001 |
| C–O$_2$ | −0.002 | −0.003 | −0.021 | 0.009 | 0.029 | −0.045 | 0.010 |
| O–H | 0.093 | 0.002 | −0.000 | 0.001 | −0.003 | −0.002 | −0.000 |
| O$_1$–C–H | 0.0 | −0.4 | −2.2 | 7.7 | 3.2 | 1.3 | −1.7 |
| O$_1$–C–O$_2$ | 0.2 | 0.7 | −0.9 | −0.4 | −2.6 | 1.1 | 4.3 |
| C–O$_2$–H | −0.1 | −0.4 | 2.1 | −2.4 | 7.4 | 5.5 | 2.9 |
| $^2A'$ state | | | | | | | |
| C–H | −0.000 | 0.104 | 0.001 | 0.006 | 0.000 | −0.001 | 0.000 |
| C–O$_1$ | −0.000 | −0.004 | −0.038 | 0.020 | 0.034 | −0.011 | 0.002 |
| C–O$_2$ | −0.003 | −0.005 | 0.043 | 0.027 | 0.006 | −0.014 | 0.003 |
| O–H | 0.095 | 0.000 | 0.000 | 0.001 | 0.001 | −0.002 | −0.000 |
| O$_1$–C–H | 0.0 | −0.3 | 4.4 | −2.3 | 6.4 | 3.4 | −3.1 |
| O$_1$–C–O$_2$ | 0.2 | 0.7 | −0.1 | −2.3 | −1.0 | −0.5 | 5.1 |
| C–O$_2$–H | −0.2 | −0.4 | −1.7 | 4.5 | −0.8 | 8.9 | 1.5 |
| $^2A''$ state | | | | | | | |
| C–H | −0.001 | 0.103 | 0.004 | 0.004 | 0.003 | −0.002 | 0.001 |
| C–O$_1$ | 0.000 | −0.005 | −0.025 | 0.021 | 0.026 | −0.041 | −0.006 |
| C–O$_2$ | −0.003 | −0.005 | 0.049 | 0.012 | −0.003 | −0.009 | −0.004 |
| O–H | 0.096 | 0.001 | 0.001 | 0.000 | −0.001 | −0.002 | 0.000 |
| O$_1$–C–H | 0.0 | −0.4 | 3.8 | −4.7 | 6.1 | 0.3 | 2.3 |
| O$_1$–C–O$_2$ | −0.3 | −0.3 | −3.1 | 6.7 | −4.5 | −0.9 | 2.1 |
| C–O$_2$–H | −0.2 | −0.4 | −1.4 | 5.1 | 5.5 | 6.5 | −2.3 |
| $CD_2O_2$ | | | | | | | |
| $^1A'$ state | | | | | | | |
| C–D | −0.001 | 0.087 | 0.021 | 0.008 | 0.002 | 0.002 | −0.000 |
| C–O$_1$ | 0.000 | −0.017 | 0.046 | 0.006 | −0.007 | −0.002 | 0.000 |
| C–O$_2$ | −0.003 | −0.002 | −0.024 | 0.050 | −0.003 | −0.019 | 0.007 |
| O–D | 0.080 | 0.001 | 0.000 | 0.001 | −0.001 | −0.002 | −0.001 |
| O$_1$–C–D | 0.0 | −0.4 | −2.0 | 4.1 | −2.5 | 5.8 | −1.3 |
| O$_1$–C–O$_2$ | 0.4 | 1.3 | −0.5 | −2.5 | −1.9 | −1.0 | 3.8 |
| C–O$_2$–D | −0.3 | −0.9 | 1.3 | 0.3 | 6.4 | 4.2 | 4.1 |
| $^2A'$ state | | | | | | | |
| C–D | 0.002 | 0.088 | 0.004 | −0.013 | 0.002 | 0.000 | −0.001 |
| C–O$_1$ | −0.000 | −0.007 | −0.039 | −0.035 | −0.015 | 0.005 | 0.001 |
| C–O$_2$ | −0.006 | −0.010 | 0.045 | −0.027 | −0.004 | −0.006 | 0.002 |
| O–D | 0.081 | −0.002 | 0.002 | −0.004 | 0.000 | −0.001 | −0.000 |
| O$_1$–C–D | −0.0 | −0.6 | 3.1 | −0.0 | −2.9 | 6.3 | −2.8 |
| O$_1$–C–O$_2$ | 0.5 | 1.2 | −0.0 | 2.2 | −1.5 | −1.4 | 4.7 |
| C–O$_2$–D | −0.4 | −0.6 | −1.6 | −1.3 | 6.5 | 5.2 | 2.6 |
| $^2A''$ state | | | | | | | |
| C–D | 0.002 | 0.087 | 0.011 | 0.013 | −0.000 | 0.002 | −0.002 |
| C–O$_1$ | 0.000 | −0.008 | −0.028 | 0.045 | −0.025 | −0.008 | 0.004 |
| C–O$_2$ | −0.006 | −0.011 | 0.048 | 0.012 | −0.002 | −0.006 | 0.003 |
| O–D | 0.082 | −0.003 | 0.004 | 0.002 | 0.000 | −0.002 | −0.001 |
| O$_1$–C–D | −0.1 | −0.7 | 2.9 | −1.0 | −4.2 | 5.5 | −1.9 |
| O$_1$–C–O$_2$ | −0.4 | −0.5 | −2.5 | 3.5 | 4.9 | −3.9 | −2.0 |
| C–O$_2$–D | −0.4 | −0.6 | −1.6 | 2.9 | 4.3 | 6.1 | 3.5 |

Bond lengths are in angstroms, angles in degrees.

Table 6
Assignment of the vibrational levels of the $^2A'$ state of $CH_2O_2$

| Vibrational progressions | | |
|---|---|---|
| A | B | C |
| 0 (S) | | |
| $\nu_3$ (S) | $\nu_4$ (W) | $\nu_6$ (W) |
| $2\nu_3$ (S) | $\nu_3+\nu_4$ (M) | $\nu_3+\nu_6$ (W) |
| $3\nu_3$ (S) | $2\nu_3+\nu_4$ (W) | $2\nu_3+\nu_6$ (W) |
| $4\nu_3$ (M) | $3\nu_3+\nu_4$ (W) | $3\nu_3+\nu_6$ (W) |
| $5\nu_3$ (W) | | $4\nu_3+\nu_6$ (W) |

Intensity is classified into S, M or W according to magnitude of FCF as follows: S: $0.23 > \text{FCF} > 0.07$, M: $0.07 > \text{FCF} > 0.03$ and W: $0.03 > \text{FCF} > 0.005$.

structure of the $^2A'$ state of $CH_2O_2$. We also show the intensity, which is classified into S (strong), M (medium) or W (weak) according to the magnitude of FCF. We find three vibrational progressions: progressions A, B and C. A vibrational progression A ($\nu_3 = 0$–$5$) has strong intensity and corresponds to the strong progression of the TIC. The vibrational progressions B ($\nu_4 = 1$ and $\nu_3 = 0$–$4$) and C ($\nu_6 = 1$ and $\nu_3 = 0$–$4$) have weak intensity. These progressions are found as shoulders of the progression A. The intensity of the progressions B and C becomes strong on the higher energy side. The shoulder becomes more distinguishable on the higher energy side. This feature is also found in the PES. The contribution of each mode to the intensity is connected with the change in the geometrical parameters by ionization. Table 1 shows that the C–$O_1$ bond lengthens, the C–$O_2$ bond shortens, the $O_1$–C–H angle becomes narrow and the C–$O_2$–H angle becomes wide. Table 4 shows that the character of the $\nu_3$ mode is a mixture of the C–$O_1$ stretching, C–$O_2$ stretching and $O_1$–C–H bending motions. Table 5 reveals that the phase of the vibrational motion is consistent with that of the molecular distortion by ionization. The magnitudes of the differences of the geometrical parameters between the ground and ionic states are larger than that of the classical half-amplitude of the $\nu_3$ mode (see Tables 1 and 5). Therefore, the vibrational excitation of the $\nu_3$ mode contributes mainly to intensity and the excitations to higher energy levels are also important. The $\nu_4$ and $\nu_6$ modes also contribute to intensity. This aspect is

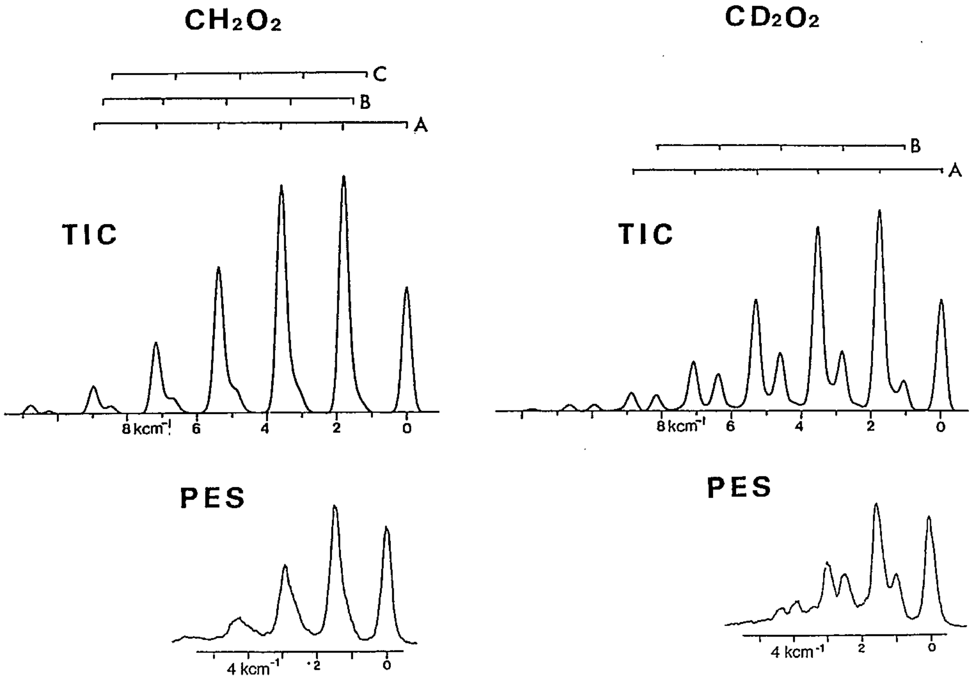

Fig. 2. The theoretical intensity curves of ionization of the $^2A'$ state with a half-width of 300 $cm^{-1}$ and the observed photoelectron spectrum by Watanabe et al. [3]. TIC: Theoretical intensity curve; PES: PE spectrum.

Table 7
Assignment of the vibrational levels of the $^2A'$ state of $CD_2O_2$

| Vibrational progressions | |
|---|---|
| A | B |
| 0 (S) | |
| $\nu_3$ (S) | $\nu_5$ (W) |
| $2\nu_3$ (S) | $\nu_3+\nu_5$ (M) |
| $3\nu_3$ (S) | $2\nu_3+\nu_5$ (M) |
| $4\nu_3$ (M) | $3\nu_3+\nu_5$ (M) |
| $5\nu_3$ (W) | $4\nu_3+\nu_5$ (W) |

Intensity is classified into S, M or W according to magnitude of FCF as follows: S: $0.23 > \mathrm{FCF} > 0.07$, M: $0.07 > \mathrm{FCF} > 0.03$ and W: $0.03 > \mathrm{FCF} > 0.005$.

ascribed to the large amplitude of the C–$O_2$–H bending motion of the $\nu_4$ and $\nu_6$ modes. The $\nu_5$ mode has a large amplitude in the C–$O_1$ stretching and $O_1$–C–H bending motions. However, the phase of those motions is not consistent with that of molecular distortion. Therefore, the $\nu_5$ mode does not contribute to the intensity.

The assignment of the vibrational levels of the $^2A'$ state of $CD_2O_2$ is shown in Table 7. We find only two vibrational progressions: progressions A and B. The vibrational progression of A ($\nu_3 = 0$–$5$) has strong intensity and that of B ($\nu_5 = 1$ and $\nu_3 = 0$–$4$) has medium intensity. The progressions A and B are separated from each other because of the distinguishable difference of the vibrational frequencies between the $\nu_3$ and $\nu_5$ modes. We should connect the contribution of these modes to the intensity with the change in the geometrical parameters. The character of the $\nu_3$ mode is a mixture of the C–$O_1$ stretching, C–$O_2$ stretching and $O_1$–C–D bending motions (see Table 4). Table 5 shows that the phase of the vibrational motion of $\nu_3$ is consistent with that of the change in the geometrical parameters. Therefore, the $\nu_3$ mode contributes mainly to intensity. The $\nu_5$ mode has a large amplitude in the C–$O_2$–D bending motion and is mixed with the $O_1$–C–D bending motion. The phase is inconsistent with the molecular distortion in the C–$O_2$–D and $O_1$–C–D bond angle.

Watanabe et al. have reported that the first band of the spectrum consisted of at least two vibrational structures. A very strong vibrational component (1486 $cm^{-1}$) for $CH_2O_2$ did not change for $CD_2O_2$. They assigned it to the C=O stretching mode. Another structure of a weak band with lower frequency (964 $cm^{-1}$) was resolved in $CD_2O_2$. They explained that the intensity of the weak band would be the sum of the O–H bending and C–H bending modes because of almost equal frequencies of the two modes in the ground state. The present calculation shows that the strong vibrational component is assigned to the vibrational excitation of the $\nu_3$ mode. The calculated vibrational frequencies of $CH_2O_2$ and $CD_2O_2$ are 1796 and 1774 $cm^{-1}$, respectively. The calcu-

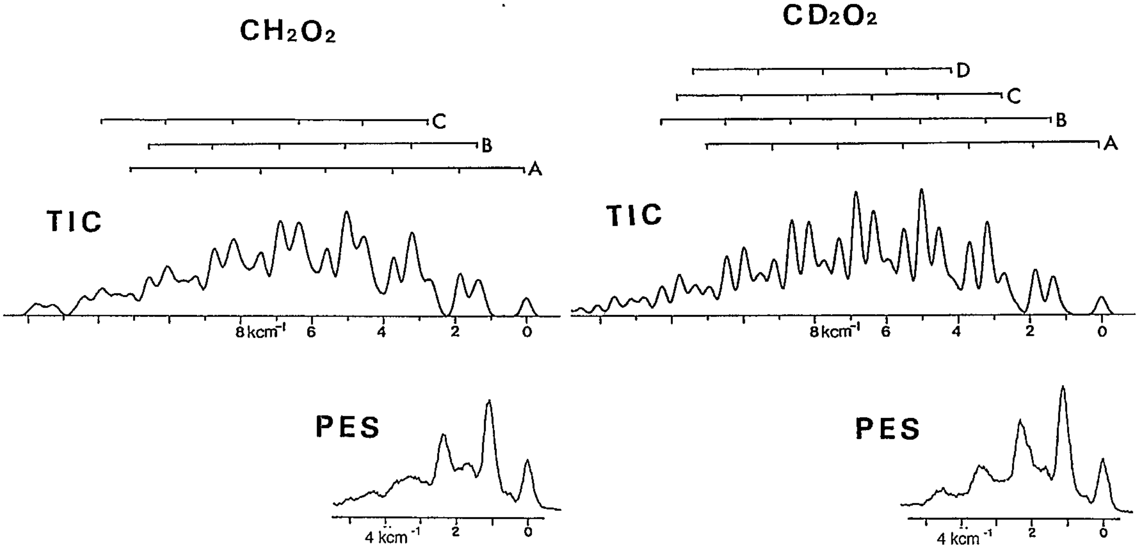

Fig. 3. The theoretical intensity curves of ionization of the $^2A''$ state with a half-width of 300 $cm^{-1}$ and the observed photoelectron spectrum by Watanabe et al. [3].

Table 8
Assignment of the vibrational levels of the $^2A''$ state of $CH_2O_2$

| Vibrational progressions | | | | | | |
|---|---|---|---|---|---|---|
| A | B | | | C | | |
| 0 (W) | | | | | | |
| $\nu_3$ (W) | $\nu_6$ (W), | $\nu_5$ (W), | $\nu_4$ (W) | | | |
| $2\nu_3$ (W) | $\nu_3+\nu_6$ (W), | $\nu_3+\nu_5$ (W), | $\nu_3+\nu_4$ (W) | $\nu_5+\nu_6$ (W), | $2\nu_4$ (W), | $\nu_4+\nu_5$ (W) |
| $3\nu_3$ (W) | $2\nu_3+\nu_6$ (W), | $2\nu_3+\nu_5$ (M), | $2\nu_3+\nu_4$ (W) | $\nu_3+\nu_5+\nu_6$ (W), | $\nu_3+2\nu_4$ (W), | $\nu_3+\nu_4+\nu_5$ (W) |
| $4\nu_3$ (W) | $3\nu_3+\nu_6$ (W), | $3\nu_3+\nu_5$ (W), | $3\nu_3+\nu_4$ (W) | $2\nu_3+\nu_5+\nu_6$ (W), | $2\nu_3+2\nu_4$ (W), | $2\nu_3+\nu_4+\nu_5$ (W) |
| $5\nu_3$ (W) | $4\nu_3+\nu_6$ (W), | $4\nu_3+\nu_5$ (W), | $4\nu_3+\nu_4$ (W) | $3\nu_3+\nu_5+\nu_6$ (W), | $3\nu_3+2\nu_4$ (W), | $3\nu_3+\nu_4+\nu_5$ (W) |
| $6\nu_3$ (W) | $5\nu_3+\nu_6$ (W), | $5\nu_3+\nu_5$ (W), | $5\nu_3+\nu_4$ (W) | $4\nu_3+\nu_5+\nu_6$ (W), | $4\nu_3+2\nu_4$ (W), | $4\nu_3+\nu_4+\nu_5$ (W) |
| | | $6\nu_3+\nu_5$ (W) | | $5\nu_3+\nu_5+\nu_6$ (W), | $5\nu_3+2\nu_4$ (W) | |

Intensity is classified into S, M or W according to magnitude of FCF as follows: M: $0.07 > \mathrm{FCF} > 0.03$ and W: $0.03 > \mathrm{FCF} > 0.005$.

lated frequencies overestimate by 19–21% compared to the observed ones. The character of the $\nu_3$ modes both of $CH_2O_2$ and $CD_2O_2$ is the C=O (C–$O_1$) stretching mode in the ground state. However, in the ionic state of $^2A'$, the character of the $\nu_3$ mode is a mixture of the C–$O_1$ stretching, C–$O_2$ stretching and $O_1$–C–H bending motions. We assign that another weak band in $CH_2O_2$ is associated to the two $\nu_4$ and $\nu_6$ modes. The $\nu_6$ mode is assigned to the O–H bending mode. The calculated vibrational frequencies of $\nu_4$ and $\nu_6$ are 1527 and 1281 $cm^{-1}$, respectively. The $\nu_4$ mode could not be assigned to the C–H bending mode. The weak band in $CD_2O_2$ is associated only to the $\nu_5$ mode, which may be assigned to the O–D bending mode. The calculated vibrational frequency is 1066 $cm^{-1}$.

Table 9
Assignment of the vibrational levels of the $^2A''$ state of $CD_2O_2$

| Vibrational progressions | | | |
|---|---|---|---|
| A | B | C | D |
| 0 (W) | | | |
| $\nu_3$ (W) | $\nu_4$ (W) | | |
| $2\nu_3$ (M) | $\nu_3+\nu_4$ (M) | $2\nu_4$ (W) | |
| $3\nu_3$ (M) | $2\nu_3+\nu_4$ (M) | $\nu_3+2\nu_4$ (M) | $3\nu_4$ (W) |
| $4\nu_3$ (W) | $3\nu_3+\nu_4$ (M) | $2\nu_3+2\nu_4$ (M) | $\nu_3+3\nu_4$ (W) |
| $5\nu_3$ (W) | $4\nu_3+\nu_4$ (M) | $3\nu_3+2\nu_4$ (M) | $2\nu_3+3\nu_4$ (W) |
| $6\nu_3$ (W) | $5\nu_3+\nu_4$ (W) | $4\nu_3+2\nu_4$ (M) | $3\nu_3+3\nu_4$ (W) |
| | $6\nu_3+\nu_4$ (W) | $5\nu_3+2\nu_4$ (W) | $4\nu_3+3\nu_4$ (W) |
| | $7\nu_3+\nu_4$ (W) | $6\nu_3+2\nu_4$ (W) | $5\nu_3+3\nu_4$ (W) |

Intensity is classified into S, M or W according to magnitude of FCF as follows: M: $0.07 > \mathrm{FCF} > 0.03$ and W: $0.03 > \mathrm{FCF} > 0.005$.

The calculated TIC of the second ionic state $^2A''$ is shown in Fig. 3. The vibrational progressions are found in the TIC. The assignments of the vibrational levels of $CH_2O_2$ and $CD_2O_2$ are shown in Tables 8 and 9, respectively. For $CH_2O_2$, we find that the $\nu_3$, $\nu_4$, $\nu_5$ and $\nu_6$ modes contribute to intensity. For $CD_2O_2$, the $\nu_3$ and $\nu_4$ modes contribute to intensity. We notice that the higher vibrational levels of the $\nu_3$ mode contribute to all vibrational progressions. The character of the $\nu_3$ mode is a mixture of the C–$O_1$ stretching, C–$O_2$ stretching, $O_1$–C–H bending, $O_1$–C–$O_2$ bending and C–$O_2$–H bending motions (see Tables 5 and 6). The phase of these motions, except for the $O_1$–C–$O_2$ bending motion, is inconsistent with that of the change in the geometry by ionization (compare Table 5 with Table 1). Thus the contribution of the $\nu_3$ mode to intensity is important.

The observed PES of the second ionic state $^2A''$ is also shown in Fig. 3. The vibrational structure of the TIC is not obviously in agreement with that of the PES. The observed separation between the first and second peaks was 1053 $cm^{-1}$, while the calculated value is 1687 $cm^{-1}$ $((\nu_3 + \nu_4)/2)$, which is overestimated by 60%. The present TIC has an intensity beyond 8 K $cm^{-1}$ (1.0 eV), while the intensity of the PES becomes weak beyond 5 K $cm^{-1}$ (0.62 eV). These situations suggest that the harmonic oscillator approximation should not be suitable for this case. Nguyen has studied the 1,3-hydrogen shifts in the $^2A''$ state at the UHF/6-31G** level [7]. He has reported the geometry of the transition state and the barrier height. The potential surface has double minima. The transition states possess $C_{2v}$ symmetry. The change in geometry between the minimum and transition structure is estimated as follows: C–H = −0.003, C–$O_1$ = −0.038 Å, C–$O_2$ = +0.053 Å, O–H = +0.316 Å, $O_1$–C–H = +11.4°, $O_1$–C–$O_2$ = −16.1° and C − $O_2$ − H = −40.1°. He has calculated the barrier height from PUMP 2/6-31G$^{**}$ + ZPE using UHF/6-31G$^{**}$ geometries. It was 0.99 eV. The direction of the change in the geometry of C–$O_1$, C–$O_2$, $O_1$–C–H, $O_1$–C–$O_2$ and C–$O_2$–H from the minimum to the transition points is inconsistent with that of the $\nu_3$ vibrational motion. Therefore, the potential energy surface corresponding to the $\nu_3$ vibrational motion should have double energy minima and the harmonic oscillator approximation should fail in the $\nu_3$ mode. The $\nu_3$ mode should have lower vibrational frequency and larger vibrational amplitude so that the intensity of ionization should have a large value in the lower energy region. We should need further investigation beyond the harmonic oscillator approximation method to obtain a more reasonable intensity curve.

Nguyen et al. have reported the 1,3-hydrogen shifts in the $^2A'$ state at the UHF/6-31G$^{**}$ level [6]. The change in geometry between the minimum and the transition structure is estimated as follows: C–H = −0.004 Å, C–$O_1$ = −0.001 Å, C–$O_2$ = +0.014 Å, O–H = +0.344 Å, $O_1$–C–H = +13.0°, $O_1$–C–$O_2$ = −23.3° and C–$O_2$–H = −36.5°. The vibrational motion of the $\nu_3$ mode of $^2A'$ is not always consistent with the motion of the distortion from the minimum geometry to the transition state. The barrier height was 1.55 eV. The TIC has an intensity below 1.0 eV. Therefore, the harmonic oscillator approximation should be reasonable for the $^2A'$ state.

## 4. Conclusion

The molecular equilibrium structure and the vibrational frequency were calculated for $^1A'$, $^2A'$ and $^2A''$ states of $CH_2O_2$ and $CD_2O_2$ within the framework of the RHF method and the harmonic oscillator approximation. We also calculated the theoretical intensity curve of ionization. An appreciable geometric change is found in the C=$O_1$ and C–$O_2$ bond length, and in the $O_1$–C–H, $O_1$–C–$O_2$ and C–$O_2$–H bond angles of both states. The C–O double bond lengthens and the C–O single bond shortens so that the distinction of the characters of single and double bonds should be meaningless in the ionic states. The $O_1$–C–H angle becomes narrow and the C–$O_2$–H angle becomes wide.

The theoretical intensity curves of the $^2A'$ state of $CH_2O_2$ and $CD_2O_2$ are in good agreement with the observed photoelectron spectra. The strong vibrational component is assigned to the vibrational excitation of the $\nu_3$ mode. The character of the $\nu_3$ mode of the ground state is assigned to the C=O (C–$O_1$) stretching mode, while that of the $^2A'$ state changes. The character of the $\nu_3$ mode is a mixture of the C–$O_1$ stretching, C–$O_2$ stretching and $O_1$–C–H bending motions. The phase of the vibrational motion is consistent with that of the molecular distortion by ionization. A weak band in $CH_2O_2$ is associated to the two modes $\nu_4$ and $\nu_6$. The $\nu_6$ mode is assigned to the O–H bending mode. The $\nu_4$ mode is not assigned to the C–H bending mode. The character is a mixture of the C–$O_1$ stretching, C–$O_2$ stretching, $O_1$–C–$O_2$ bending and C–$O_2$–H bending motions. Both $\nu_4$ and $\nu_6$ modes have a large amplitude in C–$O_2$–H bending motions. The weak band in $CD_2O_2$ is associated only with the $\nu_5$ mode and may be assigned to the C–$O_2$–D bending mode.

The vibrational progressions are found in the calculated TIC of the second ionic state $^2A''$. The higher vibrational levels of the $\nu_3$ mode contribute to all vibrational progressions. The character of the $\nu_3$ mode is a mixture of the C–$O_1$ stretching, C–$O_2$ stretching, $O_1$–C–H bending, $O_1$–C–$O_2$ bending and C–$O_2$–H bending motions. The phase of these motions, except for the $O_1$–C–$O_2$ bending motion, is consistent with that of the change in the geometry by ionization. The vibrational structure of the TIC is not in agreement with that of the PES. This should be connected to the anharmonicity of the potential surface due to the 1,3-hydrogen shift. The vibrational motion of the $\nu_3$ mode is consistent with the motion of the distortion by the 1,3-hydrogen shift. We should need further investigation beyond the harmonic oscillator approximation method to obtain a more reasonable intensity curve.

## Acknowledgement

Computation was carried out on HITAC M-68OH systems at the Center for Information Processing Education of Hokkaido University.

## References

[1] D.W. Turner, Phil. Trans. Roy. Soc. A 7 (1970) 268.

[2] I. Watanabe, Y. Yokoyama and S. Ikeda, Bull. Chem. Phys. Japan 46 (1973) 1959.

[3] I. Watanabe, Y. Yokoyama and S. Ikeda, Chem. Phys. Letters 19 (1976) 406.

[4] D.W. Turner, A.D. Baker, C. Baker and C.R. Brundle, Molecular photoelectron spectroscopy (Wiley, London, 1970).

[5] K. Kimura, S. Katsumata, Y. Achiba, T. Yamazaki and S. Iwata, Handbook of HeI photoelectron spectra of fundamental organic molecules (Halsted, New York, 1981).

[6] M.T. Nguyen, W.D. Weringa and T.K. Ha, J. Phys. Chem. 93 (1989) 7956.

[7] M.T. Nguyen, Chem. Phys. Letters 163 (1989) 344.

[8] Y.T. Chang, Y. Yamaguchi, W.H. Miller and H.F. Schaefer III, J. Am. Chem. Soc. 109 (1987) 7245.

[9] R.W. Williams and A.H. Lowrey, J. Comput. Chem. 12 (1991) 761.

[10] H. Tatewaki and S. Huzinaga, J. Comput. Chem. 1 (1980) 205.

[11] A.D. McLean and B. Liu, J. Chem. Phys. 58 (1973) 1066.

[12] T. Shoda, T. Noro, T. Nomura and K. Ohno, Intern. J. Quantum Chem. 30 (1986) 289.

[13] K. Takeshita, J. Chem. Phys. 86 (1987) 329.

[14] K. Takeshita and F. Sasaki, Library program at the Hokkaido University Computing Center, 1981 (in Japanese). GRAMOL includes the Program JAMOL3 of the RHF calculation part written by Kashiwagi et al. [13].

[15] H. Kashiwagi, T. Takada, E. Miyoshi and S. Obara, Library program at the Hokkaido University Computing Center, 1977 (in Japanese).

[16] K. Takeshita and F. Sasaki, Library program at the Hokkaido University Computing Center, 1990 (in Japanese).

[17] A. Murakami, H. Iwaki, H. Terashima, T. Shoda, T. Kawaguchi and T. Noro, Library program at the Hokkaido University Computing Center, 1986 (in Japanese).

[18] R.W. Davis, A.G. Robiette, M.C.L. Gerry, E. Bjarnov and G. Winnerwisser, J. Mol. Spectry. 81 (1980) 93.

[19] J.E. Bertie and K.H. Michaelian, J. Chem. Phys. 76 (1982) 886.

[20] Y. Morino and K. Kuchitsu, J. Chem. Phys. 21 (1952) 1809.

[21] R.C. Millikan and K.S. Pitzer, J. Chem. Phys. 27 (1957) 1305.